# X-Ray Spectroscopy With End-to-End Optimized Nanophotonic Scintillators

**William F. Li[1*], Charles Roques-Carmes[1], Zin Lin[2], Steven G. Johnson[2], and Marin Soljačić[1,3]**

[1] *Research Lab of Electronics, Massachusetts Institute of Technology, Cambridge MA 02139, USA*
[2] *Department of Mathematics, Massachusetts Institute of Technology, Cambridge MA 02139, USA*
[3] *Department of Physics, Massachusetts Institute of Technology, Cambridge MA 02139, USA*

[*] *wfli@mit.edu*

**Abstract:** We present a method for x-ray spectroscopy, combining nanophotonic scintillator inverse design with an image reconstruction algorithm. We demonstrate our pipeline on 3-energy x-ray spectroscopy, achieving 8% reconstruction error under 1% Gaussian noise © 2022 The Author(s)

Recently, a framework to model nanophotonic scintillation has been developed as a novel method for the design of nanophotonic structures to enhance scintillation [1], embodied in nanophotonic patterns at the surface of scintillators [1] and multi-layered nanophotonic scintillators [2]. This framework provides a theoretical foundation and experimental demonstration for the application of nanophotonic methods to the design of scintillators, showing enhancement and control of scintillation light by nanophotonic design. Particularly relevant for our work is the new implication that scintillators can be designed by existing techniques in nanophotonics, such as inverse design and topology optimization. Our work integrates this novel nanophotonic scintillation framework with the previously developed technique of end-to-end nanophotonic inverse design [3] to develop a layered nanophotonic scintillator for x-ray spectroscopy. We demonstrate our method on the problem of 3-energy x-ray spectroscopy.

End-to-end nanophotonic optimization is a design technique in which a nanophotonic structure and an image reconstruction algorithm are optimized jointly to best capture and represent a ground-truth source. The advantage of end-to-end optimization of nanophotonic scintillators is two-fold: first, the design of optimized nanophotonic scintillators gives us the potential to capture a stronger, more noise-robust signal from lower-intensity x-rays [1]. Second, by combining our imaging system with a computational reconstruction algorithm, we increase the amount of information that can be extracted from the incoming signal. With a computational reconstruction algorithm, the image on the detector no longer has to be suitable for human viewing, as the reconstruction algorithm is much more flexible in handling images. Therefore, in addition to the "physical processing" being performed by the nanophotonic scintillator, our reconstruction algorithm adds on computational processing, allowing the extraction of even more data from the same incoming signal.

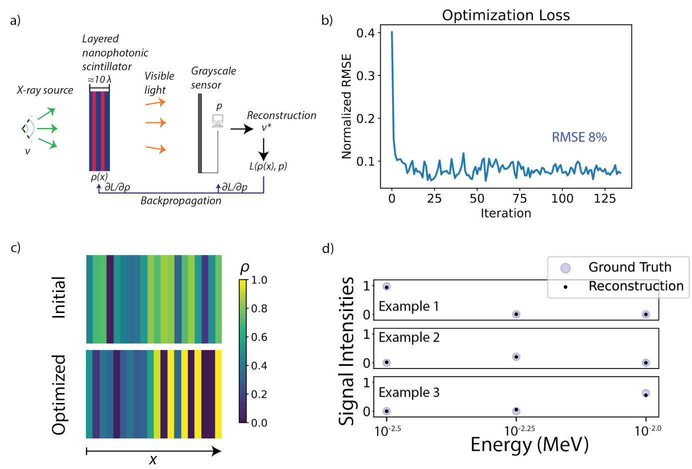


Fig. 1. Optimization pipeline. (a) Schematic of the end-to-end framework for x-ray spectroscopy. We jointly optimize over the structure and the reconstruction parameters. (b) Optimized normalized root-mean-square error (NRMSE) is plotted against the iteration number of optimization steps. (c) Initial and optimized structures, the color indicating the scintillator density $\rho$ and $x$ being position in the layered stack; the stack is discretized into 20 degrees of freedom. (d) Three example reconstructions. In each example, the reconstruction identifies the energy of the ground-truth signal and its intensity.

We consider a nanophotonic scintillator made up of two alternating materials: a scintillator and silica ($SiO_2$).

Such structures have recently been realized to demonstrate Purcell-enhanced x-ray scintillation [4]. We treat the one-dimensional scintillator density $\rho(x)$ at each discretized position $x$ in the stack as a degree of freedom in the optimization, where $0 \leq \rho(x) \leq 1$ at each position $x$, $\rho(x) = 0$ corresponding to having full $SiO_2$ at the location and $\rho(x) = 1$ corresponding to having full scintillator; in our example (Fig. 1(c)), the entire length is discretized into 20 degrees of freedom. We choose the refractive index of the scintillator to be around 2.3, corresponding to cadmium tungstate. Our simulation setup is shown in Fig. 1(a): an x-ray point source (characterized by energy $h\nu$) is incident on a structure described by a scintillation profile $\rho(x)$. The intensity profile on the detector is modeled via near-to-far field transformation (integrated over each detector pixel). We choose a flexible Elastic-Net reconstruction algorithm to reconstruct the ground-truth spectral data from the image generated by our nanophotonic structure. Elastic-Net is parametrized by the coefficients of $l_1$ and $l_2$ normalization, which we denote as $p_1$ and $p_2$ respectively. We use the fast iterative soft-thresholding algorithm (FISTA) to solve the Elastic-Net problem. The reconstructed spectral data $\tilde{\mathbf{u}}$ is the output of the FISTA reconstruction. The FISTA reconstruction is obtained via the LASSO- and Tikhonov-regularized inverse scattering problem:

$$\tilde{\mathbf{u}} = \mathrm{argmin}_u \; \|\mathbf{G}u - \mathbf{v}\|^2 + p_1||u||_1 + p_2||u||_2, \tag{1}$$

where $\tilde{\mathbf{u}}$ is the reconstructed object, $\mathbf{v}$ the raw image, $\mathbf{G}$ the measurement matrix, and $||.||_1$ the $L_1$-norm. The measurement matrix $\mathbf{G}$ is a function of the geometrical parameters of the nanophotonic stack and is optimized to be suitable for Elastic-Net Reconstruction. We choose Elastic-Net for its flexibility: based on the properties of the ground-truth $u$, our end-to-end optimization algorithm finds different settings of $p_1$ and $p_2$ to minimize reconstruction error. For instance, when $u$ is sparse, the optimization algorithm generally emphasizes the $l_1$ regularization term, increasing $p_1$ and decreasing $p_2$ to approximate LASSO regularization. This flexibility makes Elastic-Net suitable for a far wider class of problems than either LASSO- or Tikhonov- regularized reconstruction alone.

We use our pipeline, shown in Fig. 1(a), to solve the problem of x-ray spectral sensing (Fig. 1(d)). We compute gradients for each iteration through backpropagation and the adjoint method. In the forward pass, an x-ray source is incident upon a nanophotonic scintillator structure, which absorbs the x-rays and emits visible light scattered by the structure, which is detected by the sensor and reconstructed into an estimated ground truth. In the backward pass, we backpropagate through Elastic-Net regression then compute the structure gradients using the adjoint method. We use Adam to update the structure and reconstruction parameters from the gradients. The optimized structures in Fig. 1(c) (right) show the map of scintillator density $\rho$ in the design region. Our incident light comes from the $-\hat{x}$ direction in relation to the structures (left of the page). $\rho$ within our design region is constrained to be between $\rho = 0$ (all $SiO_2$) and $\rho = 1$ (all scintillator). We train our system to reconstruct ground truths $u$ consisting of a single energy $h\nu$. In the training set, we allow $\nu$ to take on three possible values, so each training example $u$ is a length-3 vector with one nonzero value. Our optimized nanophotonic scintillator stack achieves reconstruction with 8% normalized RMS error (NRMSE). In comparison, a random nanophotonic structure under 1% noise performs at 16% NRMSE upon optimizing the reconstruction parameters only.

Directly modeling a scintillator requires many expensive simulations of random dipoles within the scintillating material. To work around this, we use a recently-developed electromagnetic reciprocity-based framework [1], described more generally in [5]. We perform our simulation in two steps: first, we compute the x-ray absorption profile of the scintillator from an x-ray source of several possible energies; second, we compute the fields in the scintillator from visible light sources at each sensor pixel. By integrating the fields together with the x-ray absorptions, we obtain the signal observed by each detector pixel.

In conclusion, we have demonstrated end-to-end optimized nanophotonic scintillators for x-ray spectroscopy. Our work has great promise in the design of x-ray imagers with reduced x-ray exposure, with applications to medical computed tomography scanners and radiography.

## References


[1] Charles Roques-Carmes et al. "A framework for scintillation in nanophotonics". In: *Science* 375.6583 (2022), eabm9293.

[2] Yaniv Kurman et al. "Photonic-crystal scintillators: Molding the flow of light to enhance X-ray and $\gamma$-ray detection". In: *Physical Review Letters* 125.4 (2020), p. 040801.

[3] Zin Lin et al. "End-to-end nanophotonic inverse design for imaging and polarimetry". In: *Nanophotonics* 10.3 (2021), pp. 1177–1187.

[4] Neta Lahav et al. "Purcell enhancement of X-ray scintillation". In: *CLEO: Science and Innovations*. Optica Publishing Group. 2022, SM3K–7.

[5] Wenjie Yao et al. "Trace formulation for photonic inverse design with incoherent sources". In: *Structural and Multidisciplinary Optimization* 65.11 (2022), pp. 1–16.